AD-A091 252 HARRY DIAMOND LABS ADELPHI MD F/G 20/2
OPTICAL SPECTRA OF YB(3+) IN CRYSTALS WITH SCHEELITE STRUCTURE.--ETC(U)
SEP 80 E A BROWN
UNCLASSIFIED HDL-TR-1932 NL

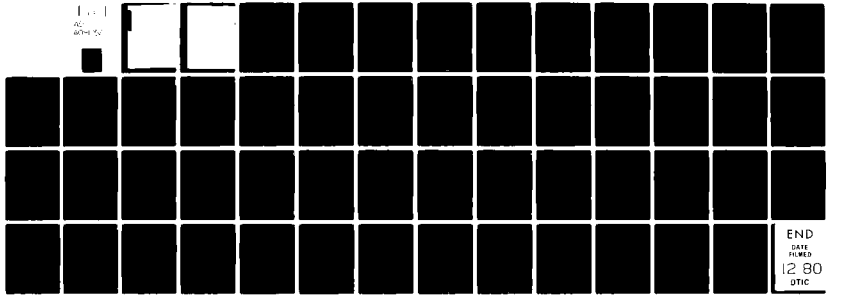

END
DATE FILMED
12 80
DTIC

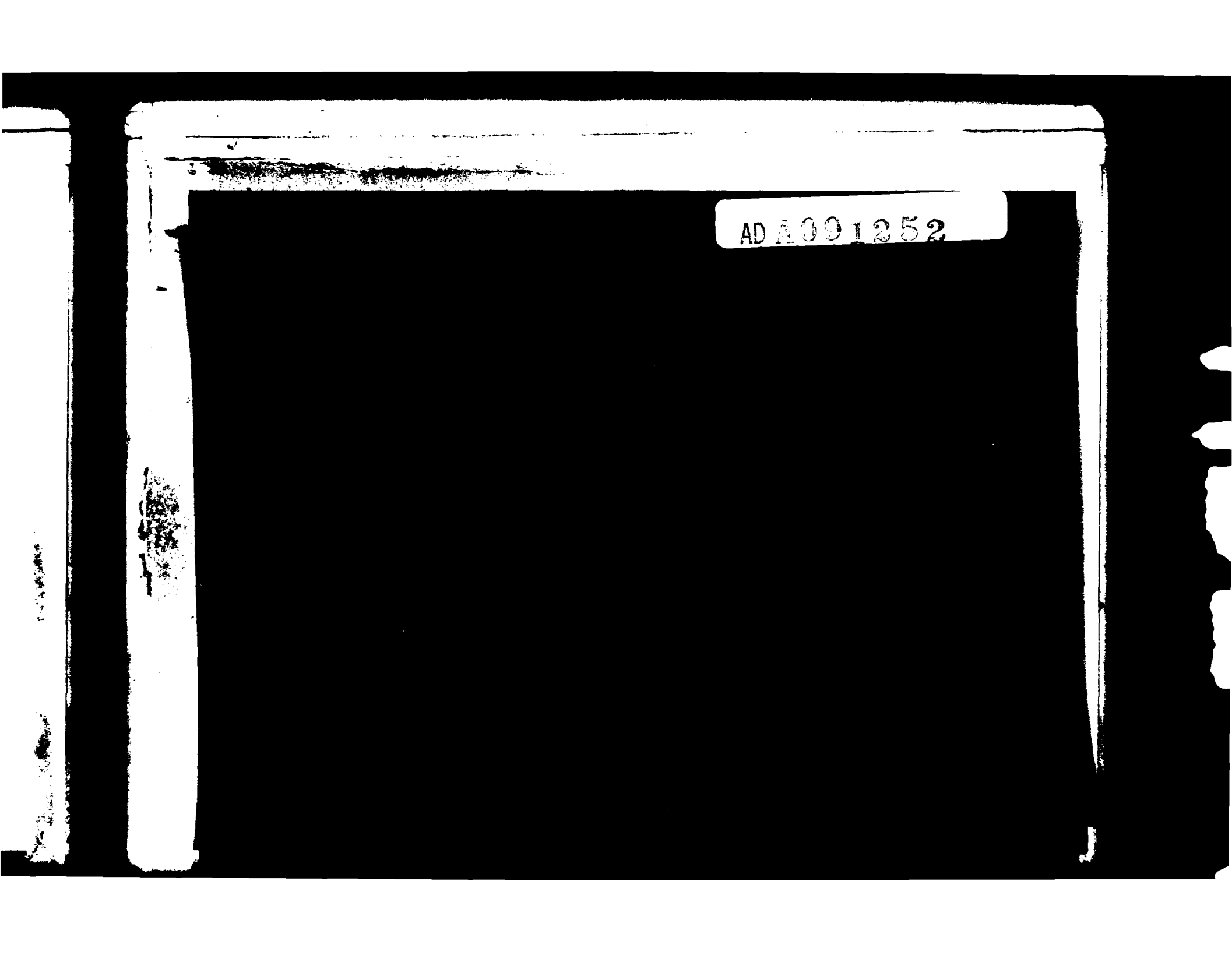

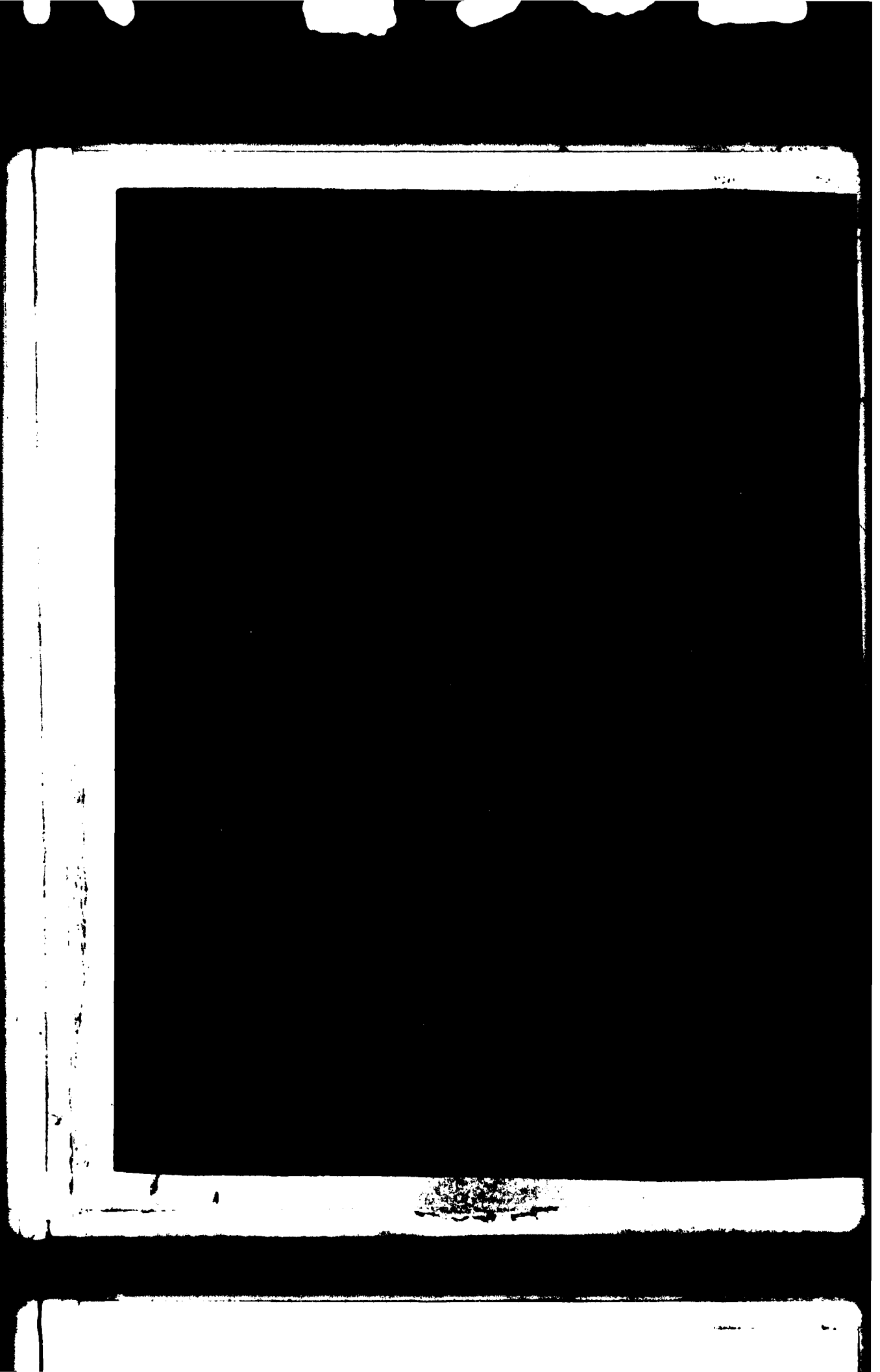

UNCLASSIFIED

SECURITY CLASSIFICATION OF THIS PAGE (When Data Entered)

14

REPORT DOCUMENTATION PAGE

READ INSTRUCTIONS BEFORE COMPLETING FORM

1. REPORT NUMBER: HDL-TR-1932
2. GOVT ACCESSION NO.: AD-A091252
3. RECIPIENT'S CATALOG NUMBER:

6

4. TITLE (and Subtitle): Optical Spectra of Yb^{3+} in Crystals with Scheelite Structure, I. Explanation of the Spectra.

5. TYPE OF REPORT & PERIOD COVERED: Technical Report

6. PERFORMING ORG. REPORT NUMBER:

10

7. AUTHOR(s): Edward A. Brown

8. CONTRACT OR GRANT NUMBER(s):

9. PERFORMING ORGANIZATION NAME AND ADDRESS
Harry Diamond Laboratories
2800 Powder Mill Road
Adelphi, MD 20783

10. PROGRAM ELEMENT, PROJECT, TASK AREA & WORK UNIT NUMBERS

11. CONTROLLING OFFICE NAME AND ADDRESS
US Army Materiel Development and Readiness Command
Alexandria, VA 22333

11

12. REPORT DATE: Sep[redacted] 1980

13. NUMBER OF PAGES: 53

14. MONITORING AGENCY NAME & ADDRESS (if different from Controlling Office)

12 54

15. SECURITY CLASS. (of this report): UNCLASSIFIED

15a. DECLASSIFICATION/DOWNGRADING SCHEDULE

16. DISTRIBUTION STATEMENT (of this Report)

Approved for public release; distribution unlimited.

17. DISTRIBUTION STATEMENT (of the abstract entered in Block 20, if different from Report)

18. SUPPLEMENTARY NOTES

AIF appropriation: 21X4992.06LA 6L S18129
HDL Project: 001A14

19. KEY WORDS (Continue on reverse side if necessary and identify by block number)

Crystal fields
Scheelites
Rare earth
Laser materials
Group theory
Vibronics
Optical spectra

20. ABSTRACT (Continue on reverse side if necessary and identify by block number)

The optical and Zeeman spectra are reported for Yb^{3+} in nine single crystals of the Scheelite family at temperatures varying between 1.9 and 300 K and impurity ion concentration varying between 0.05 and 4 percent. The scheelite crystals examined were $CaWO_4$, $CaMoO_4$, $SrWO_4$, $SrMoO_4$, $PbWO_4$, $PbMoO_4$, $CdMoO_4$, $BaWO_4$, and $LiYF_4$. The Yb^{3+} ion substitutes for the cation and experiences a crystalline electric field of S_4 point symmetry. The spectra were

DD FORM 1 JAN 73 1473 EDITION OF 1 NOV 65 IS OBSOLETE

UNCLASSIFIED

SECURITY CLASSIFICATION OF THIS PAGE (When Data Entered)

163050

20. Abstract (Cont'd)

found to be highly structured containing the S_4 electronic transitions, concentration dependent lines originating from low symmetry sites caused by lattice defects, and features tentatively identified as vibronic transitions. Vibronic selection rules for Yb^{3+} in scheelite, which belongs to the C_{4h}^6 space group, have been calculated. Identification of the S_4 spectral lines allowed the energy level schemes for Yb^{3+} in the nine scheelites to be determined.

CONTENTS

FIGURES

TABLES

1. INTRODUCTION

Although many features of the spectra of rare-earth impurity ions in solids are successfully described by crystal-field theory, there is poor agreement between crystal-field parameters determined from optical spectra and those calculated from the basic properties of the crystal host and the rare-earth impurity ion.[1] Attempts have been made to explain rare-earth ion spectra by considering overlap and exchange with ligand ions,[2-4] but additional work will be necessary before this approach can be properly evaluated. To provide information that may prove useful for obtaining an improved description of rare-earth ion spectra in solids, we have investigated the optical spectra of trivalent ytterbium (Yb^{3+}) in nine isomorphic crystals with scheelite structure. In this report, the experimental part of this investigation is presented. An analysis of the results from the point of view of crystal-field theory is given in an accompanying report.[5]

Scheelite is a family of tetragonal crystals belonging to the space group $C_{4h}^6(I4_1/a)$. The scheelites that we have used in this study were cadmium molybdate ($CdMoO_4$), calcium tungstate ($CaWO_4$), calcium molybdate ($CaMoO_4$), strontium tungstate ($SrWO_4$), strontium molybdate ($SrMoO_4$), lead tungstate ($PbWO_4$), lead molybdate ($PbMoO_4$), barium tungstate ($BaWO_4$), and lithium yttrium fluoride ($LiYF_4$). The lattice parameters[6-9] for

---

[1] *H. J. Van Vleck, J. Phys. Chem. Solids, 27 (1966), 1047.*

[2] *M. M. Ellis and D. J. Newman, J. Chem. Phys., 47 (1967), 1986.*

[3] *S. S. Bishton, M. M. Ellis, D. J. Newman, and J. Smith, J. Chem. Phys., 47 (1967), 4133.*

[4] *R. E. Watson and A. J. Freeman, Phys. Rev., 156 (1967), 251.*

[5] *E. A. Brown, Optical Spectra of Yb^{3+} in Crystals with Scheelite Structure, II. Crystal Field Calculations and a Phenomenological Crystal Field Model, Harry Diamond Laboratories HDL-TR-1934 (September 1980).*

[6] *H. E. Swanson, N. T. Gilfrich, and M. I. Cooke, National Bureau of Standards Circular 539, 6 (1956).*

[7] *H. E. Swanson, N. T. Gilfrich, and M. I. Cooke, National Bureau of Standards Circular 539, 7 (1957).*

[8] *A. Zalkin and D. H. Templeton, J. Chem. Phys., 40 (1964), 501.*

[9] *J. Leciejewicz, Z. Kristallogr., 121 (1965), 158.*

these crystals are listed in table 1. These scheelites have four molecular units in a unit cell. In the tungstates and the molybdates, the divalent cations are coordinated with eight oxygens, each of which is a member of a $(WO_4)^{2-}$ or $(MoO_4)^{2-}$ complex. Yb^{3+} ions substituted in an undistorted divalent cation site are optically and magnetically equivalent and have S_4 point symmetry. In the $LiYF_4$, the Yb^{3+} ions replace the trivalent yttrium (Y^{3+}) ions and coordinate with eight fluorines that are members of the $(LiF_4)^{3-}$ complex. Point symmetries are the same as in the other scheelites.

TABLE 1. LATTICE PARAMETERS OF SCHEELITE CRYSTALS

Crystal	c axis (Å)	a axis (Å)
$CdMoO_4$*	11.194	5.1554
$CaWO_4$†	11.376(3)	5.243(2)
$CaMoO_4$*	11.43	5.226
$SrWO_4$*	11.951	5.4168
$SrMoO_4$*	12.020	5.3944
$PbWO_4$*	12.046	5.4616
$PbMoO_4$‡	12.1065(39)	5.4312(16)
$BaWO_4$*	12.720	5.6134
$LiYF_4$§	10.733(2)	5.1668(3)

*Values from H. E. Swanson, N. T. Gilfrich, and M. I. Cooke, National Bureau of Standards Circular 539, 6 (1956); 7 (1957).

†Values from A. Zalkin and D. H. Templeton, J. Chem. Phys., 40 (1964), 501.

‡Values from J. Leciejewicz, Z. Kristallogr., 121 (1965), 158.

§Values from J. S. King, University of Michigan, private communication.

The optical spectrum of Yb^{3+} in $CaWO_4$ has been investigated by Pappalardo and Wood[10] and by Jones.[11] Their results can be described by reference to the energy level diagram of the $4f^{13}$, ^2F states of Yb^{3+}

[10] R. Pappalardo and D. L. Wood, J. Mol. Spectrosc., 10 (1963), 81.
[11] G. R. Jones, J. Chem. Phys., 47 (1967), 4347.

shown in figure 1. The ^2F state is split approximately 10,000 cm^{-1} by the spin-orbit interaction; the crystal-field interaction causes a further splitting in the crystal of about 500 cm^{-1} for the $^2F_{7/2}$ multiplet and about 400 cm^{-1} for the $^2F_{5/2}$ multiplet. Pappalardo and Wood observed energies and polarization of the absorption transitions A, B, and C and the fluorescence transitions D, E, F, and G at low temperatures. They noted that considerable structure or satellites were associated with each absorption transition.

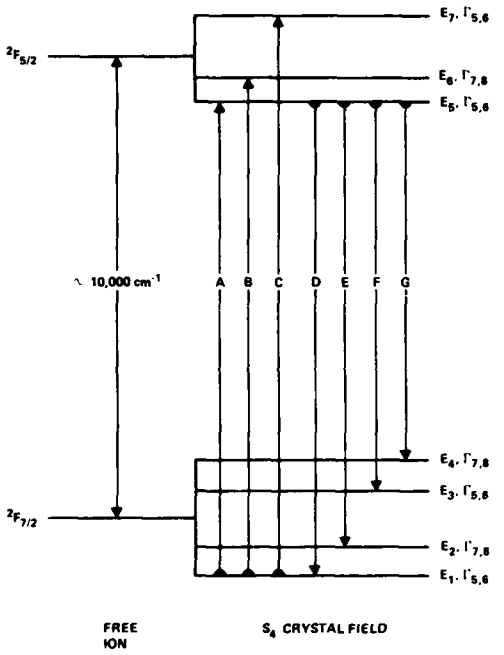

Figure 1. Energy levels of $4f^{13}$, ^2F states of Yb^{3+} free ion and ion in S_4 crystal field. (The irreducible representations indicated were determined for Yb^{3+} in the scheelites considered in this work. An interchange of the representations shown for energy levels E_3 and E_4 is allowed by the experimental data.)

The absorption spectra of a number of samples grown with sodium (Na) for charge compensation were examined by Jones. He found that only the satellites with energies below those of the A transition were absent in compensated crystals. Jones determined the irreducible representations of the states (in the notation of Koster et al[12]) to be as shown in

[12] *G. F. Koster, J. O. Dimmock, R. G. Wheeler, and H. Statz, Properties of the Thirty-Two Point Groups, Massachusetts Institute of Technology Press, Cambridge, MA (1963).*

figure 1. He calculated least-squares-fit crystal-field parameters for Yb^{3+} in $CaWO_4$. Jones attributed the remaining structure in the spectra to vibronic components of the A transition.

However, Kiel and Crane[13] have raised objections both to this explanation and to one concerning the proximity of the Yb^{3+} ions to compensation ions or vacancies. They argue that both identifications are inconsistent with the observed polarization of the spectra and also with the results of their microwave-optical double resonance experiments.

In this work, we reexamine the spectrum of Yb^{3+} in $CaWO_4$, with particular attention to the fluorescence spectrum since details on this spectrum were not published by Pappalardo and Wood.

The electron-paramagnetic-resonance spectrum also has been investigated for Yb^{3+} in the scheelites considered here.[14,15] From these studies, it was concluded that the Yb^{3+} ions are located predominantly in tetragonal sites with S_4 point symmetry and, except for barium tungstate ($BaWO_4$), their ground states are unambiguously $\Gamma_{5,6}$. We have obtained the optical absorption, fluorescence, and Zeeman spectra of the same crystals used for electron paramagnetic resonance (EPR) measurements, as well as others with higher concentration of Yb^{3+}. In section 2, the procedure used to obtain these spectra is described, and the character of the spectra is compared with that obtained for $CaWO_4:Yb^{3+}$. In section 3, the polarization of the spectra and electric dipole selection rules are used to determine the irreducible representation of the states. Selection rules for vibronic transitions are obtained and used in a discussion of possible causes for the structure observed in the spectra.

---

[13] *A. Kiel and G. R. Crane, J. Chem. Phys., 48 (1968), 3751.*
[14] *U. Ranon and V. Volterra, Phys. Rev., 134 (1964), A1483.*
[15] *J. P. Sattler and J. Nemarich, Phys. Rev. B, 1 (1970), 4249.*

2. EXPERIMENTAL PROCEDURE AND MEASUREMENTS

2.1 Crystals

Samples used in this work were single crystals grown from oriented seeds by the Czochralski method at this laboratory,[16] with the exception of the $LiYF_4$ samples.* For the tungstates and the molybdates, the melt composition consisted of the scheelite powder (crystal grade) Yb_2O_3 (99.9 percent), and for the charge compensation, sodium tungstate ($NaWO_4$) or sodium molybdate ($NaMoO_4$) as appropriate (99.99 percent). Crystal composition was based on melt composition and was estimated by the distribution coefficients of Nassau and Loiacano.[17] The concentrations of ytterbium in the melts ranged from 0.05 atomic percent to several percent. Most of the crystals were clear and free from optical imperfections, but some evidenced strain when viewed in polarized light. The $CdMoO_4$ and some of the $CaMoO_4$ samples were bluish green, the $PbWO_4$ and $PbMoO_4$ crystals had a yellowish cast, and all other crystals were colorless. The crystals were annealed in oxygen at temperatures between 1000 and 1300 C for 24 hr.

The crystals were cut and polished rectangular parallelopipeds with typical dimensions of 0.25 × 0.25 × 0.6 in. (0.6 × 0.6 × 1.5 cm). The crystal c axis was determined by x-ray or by viewing the crystal in polarized light. The long dimension of the crystal was cut perpendicular to the crystal c axis so that σ (electric vector, E, perpendicular to the c axis) and π (E parallel to the c axis) spectra could be taken without remounting the crystal.

---

[16] *R. M. Curnutt, Czochralski Growth of Tungstate and Molybdate Scheelites, Harry Diamond Laboratories HDL-TM-70-8 (July 1970).*

[17] *K. Nassau and G. M. Loiacano, J. Phys. Chem. Solids, 24 (1963), 1503.*

**$LiYF_4$ samples were grown by A. Linz, Massachusetts Institute of Technology.*

2.2 Apparatus

The majority of the spectra were taken by mounting the samples in a cold-finger type of cryostat with quartz windows and by using both liquid helium and liquid nitrogen as coolants. The actual sample temperature was measured by using a germanium resistor. The temperatures obtained were 26 K by using liquid helium and 84 K by using liquid nitrogen. To obtain measurements at still lower temperatures, an immersion dewar was used with liquid helium. The liquid surface was pumped to reduce the temperature below the helium lambda point and thus eliminate bubbling. The temperature for these measurements was 1.9 K.

Most of the measurements were made with a Jarrell Ash 1-m Ebert monochrometer. Its grating was blazed at 1 μm in first order, and the signal was detected by a cooled RCA 7102 photomultiplier. For some measurements, a Cary 14 scanning spectrophotometer was used.

The wavelengths of the spectral lines were determined by superimposing known reference lines from a small xenon gas discharge lamp. In addition to this determination, evenly spaced pulses were superimposed on the recorder output by an optical encoder mounted coaxially on the drive mechanism of the spectrometer. The pulses subdivided the regions between the reference lines and enabled a determination of the wavelength of any point on the spectrum to an accuracy of about 1 Å, well within the actual width of most of the lines.

Excitation of the spectra was provided mainly by tungsten-halogen lamps, although some of the fluorescence measurements were taken by using a mercury-xenon arc. Narrow and broad band-pass filters, water and neutral density filters, and polarizing filters were used to reduce stray light, to control excess heating of the samples, and to take both excitation and polarized spectra.

The magnet used for the Zeeman measurements was a 22-in. (55.9-cm) Varian electromagnet with a 1.5-in. (3.8-cm) air gap and a maximum field of about 32 kG. The magnet had removable axial plugs, which allowed measurements with the optical path to be parallel and perpendicular to the field.

3. ANALYSIS OF SPECTRA

3.1 Spectra of $CaWO_4$:Yb

The absorption spectrum of $CaWO_4$:Yb at 1.9 K is shown in figure 2. This spectrum was obtained by using a crystal prepared with 0.1 atomic percent Yb and 1.5 atomic percent Na (for charge compensation) in the melt. The spectrum is similar to that reported by Jones[11] for a sample prepared with an eight-to-one ratio of Na to Yb in the melt. The polarization of this spectrum was in agreement with the results by Jones.

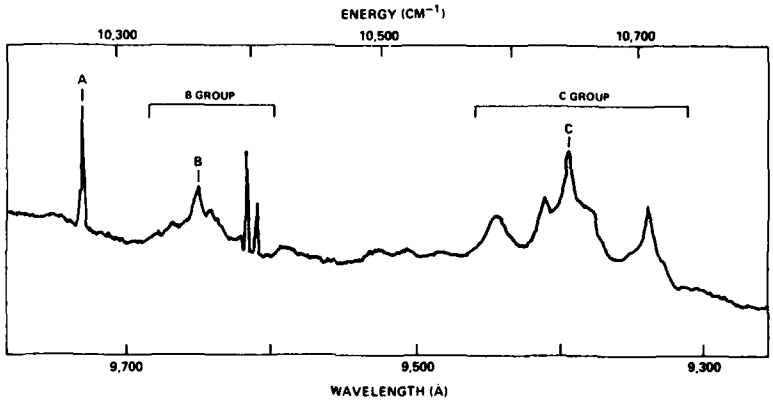

Figure 2. Absorption spectrum of $CaWO_4$:0.1% Yb and 1.5% Na at 1.9 K.

[11] *G. R. Jones, J. Chem. Phys., 47 (1967), 4347.*

3.1.1 Polarization Effects

Data taken with a polarizing filter in two positions yielded a σ spectrum and a π spectrum. The lines labeled A and B are σ and π; the C group is pure σ. An axial spectrum was found to be identical to the σ spectrum, thus demonstrating according to the theory of Sayre, Sancier, and Freed[18] that the transitions are primarily electric dipole.

As shown in figure 1, three absorption transitions are possible from the ground state to the J = 5/2 multiplet for Yb^{3+} in a crystal field of S_4 point symmetry. Since the ground state is known to be $\Gamma_{5/6}$ from EPR measurements,[14] the polarizations of the transitions to the upper states may be determined from the group representations of the upper states and the electromagnetic field. The selection rules for both electric and magnetic dipole transitions are summarized in table 2.

TABLE 2. POLARIZATIONS OF ALLOWED ELECTRIC AND MAGNETIC DIPOLE RADIATIVE TRANSITIONS BETWEEN STATES WITH S_4 IRREDUCIBLE REPRESENTATIONS

	Γ_5	Γ_6	Γ_7	Γ_8
Γ_5	σ_m	σ_e, π_m	π_e	σ_e, π_m
Γ_6		σ_m	σ_e, π_m	π_e
Γ_7			σ_m	σ_e, π_m
Γ_8				σ_m

Note: The electric vector is perpendicular to the crystal c axis for σ polarization and parallel for π polarization. The subscripts e and m denote electric and magnetic dipole transitions, respectively.

Since each of the two broad and structured groups of lines (B and C) have uniform polarization characteristics, they each probably contain an S_4 transition from the ground state, and the sharp A line is the remaining S_4 transition. In table 3, the energies are listed for

[14] *U. Ranon and V. Volterra, Phys. Rev., 134 (1964), A1483.*

[18] *E. V. Sayre, K. M. Sancier, and S. Freed, J. Chem. Phys., 23 (1955), 2060.*

the A line and the approximate centroids of the B and C groups of lines. The energies are quoted in units of inverse centimeters (cm^{-1}) in vacuum, whereas the values quoted by Jones are in cm^{-1} in air. The representations of the upper states as determined by Jones from the polarizations are shown in figure 1. The π component of the A line is believed to be a magnetic dipole transition.[11,13]

3.1.2 Concentration Effects

The spectrum of $CaWO_4$:Yb grown with concentrations of 0.5 and 1.0 atomic percent ytterbium with sodium for charge compensation in a ratio of four to one to ytterbium was examined. On the low energy side of the A line, five or six small, well-defined lines appeared as the concentration was raised. These and other concentration dependent lines were due probably to Yb^{3+} ions near charge compensating impurities, vacancies, or other charge defects, the number of which is expected to increase as the ytterbium concentration is increased. These lines were in agreement with lines found by Jones in the same region. The slight shoulder on the low energy side of the A line came up with concentration. This low energy satellite structure on the A line was present in all the crystals studied when the ytterbium concentration was sufficiently high. The structure on the B transition group of lines grew relative to the center line of the group with increasing ytterbium concentration, but the very sharp lines on the high energy side did not. The low intensity structure between the B and C groups also maintained a fairly constant amplitude with respect to the B line as the ytterbium concentration was increased. The lines of the C group showed a profound change with ytterbium concentration. The satellites on both sides of the central peak grew between 50 and 100 percent with increasing ytterbium concentration.

---

[11] *G. R. Jones, J. Chem. Phys., 47 (1967), 4347.*
[13] *A. Kiel and G. R. Crane, J. Chem. Phys., 48 (1968), 3751*

TABLE 3. ENERGIES (cm^{-1} IN VACUUM) FOR SPECTRAL LINES OF Yb^{3+} IN NINE SCHEELITE CRYSTALS

S_4 line	$LiYF_4$	$CdMoO_4$	$CaWO_4$	$CaMoO_4$	$SrWO_4$	$SrMoO_4$	$PbWO_4$	$PbMoO_4$	$BaWO_4$	Line shape and strength	
										Perpendicular, σ	Parallel, π
Absorption											
A'	--	10,046	10,059	--	10,109	10,099	10,106	10,088	10,124	vd,vw	vd,vw
B'	--	--	10,155	10,155	10,166	10,157	--	--	10,156	vd,vw	vd,vw
A	10,288	10,267	10,274	10,263	10,264	10,251	10,260	10,246	10,254	sh,s	sh,m
B	10,409	10,381	10,363	10,349	10,318	10,313	10,314	10,309	10,291	d,m	d,s
C	10,547	10,653	10,645	10,628	10,605	10,601	10,604	10,586	10,549	d,s	Not observed
Fluorescence											
D'	--	--	--	--	--	--	--	--	10,291	sh,m	d,w
D	10,288	10,267	10,274	10,263	10,264	10,251	10,260	10,246	10,254	sh,m	sh,w
E'	--	10,158	10,145	--	10,172	10,160	10,148	10,152	10,163	sh,w	sh,w
E	10,072	10,041	10,060	10,070	10,114	10,097	10,098	10,086	10,127	sh,m	sh,s
F'	10,045?	--	--	9,988	9,987	9,982	--	9,977	10,000	d,w	d,m
F	9,917	9,882	9,908	9,906	9,932	9,918	9,937	9,919	9,963	d,m	d,m
G'	--	9,896	9,857	9,881	--	9,894	--	9,900	--	d,vw	Not observed
G	9,809	9,778	9,785	9,790	9,818	9,831	9,831	9,840	9,846	d,m	d,m

Note: The S_4 lines A to G are identified as transitions from levels E_1 and E_5 shown in figure 1. The lines A' to G' refer to corresponding transitions from levels E_2 and E_6 shown in figure 1. The line shape and the strength of the σ and π spectra are denoted as sh--sharp, d--diffuse, vd--very diffuse, s--strong, m--medium, w--weak, and vw--very weak.

The only additional concentration dependent features of the spectrum were a few weak diffuse lines at about 9100 Å. We believe that the lines are not related to the S_4 spectrum since the analysis presented in the accompanying report[5] shows them to be inconsistent with this spectrum.

The fluorescence spectrum of $CaWO_4$:Yb at 1.9 K is shown in figure 3. The same crystal was used as for the spectrum of figure 2. The D line corresponds to the A line observed in absorption. The energies of the indicated approximate centroids of the three broad and structured groups of lines E, F, and G are given in table 3. The lines designated D', E', F', and G' refer to transitions from level E_6 to levels E_1, E_2, E_3, and E_4 in figure 1. All of the lines were observed in both σ and π polarization. The E group (plus and minus about 100 cm^{-1} from the indicated centroid) was considerably stronger in π than in σ. The other lines were stronger in σ. To reduce the effects of depolarization of the fluorescence due to scattering, a sample was coated completely with aquadag (a suspension of graphite in ethanol), except for a small space through which to excite the crystal and another space on a perpendicular face to allow the emission to exit to the spectrometer. This coating reduced the σ component of the E line with the E, F, and G lines all having approximately equal intensity in σ. The π components of both the F and G lines also were sharply reduced with intensities about 5 percent or less of the π component of the E line. Undoubtedly, some depolarization effects were still present, and it was not possible to unambiguously determine whether either of the remaining π components of the F and G lines was spurious.

---

[5] *E. A. Brown, Optical Spectra of Yb^{3+} in Crystals with Scheelite Structure, II. Crystal Field Calculations and a Phenomenological Crystal Field Model, Harry Diamond Laboratories HDL-TR-1934 (September 1980).*

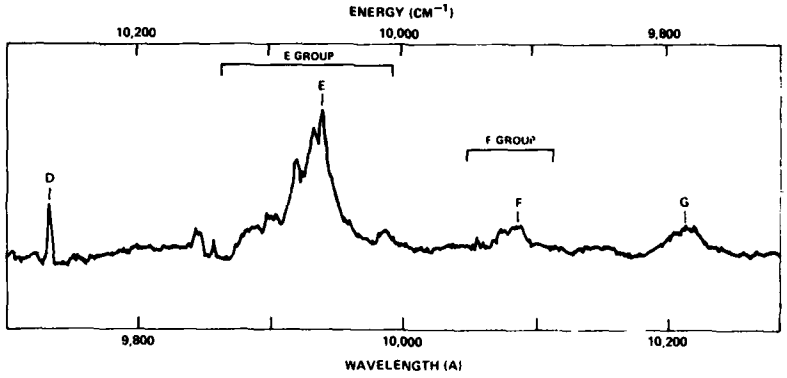

Figure 3. Fluorescence spectrum of $CaWO_4$:0.1% Yb and 1.5% Na at 1.9 K.

The effect of concentration on the fluorescence spectra of $CaWO_4$:Yb was measured in the samples described above. Unlike the absorption spectra, there is very little change of the relative intensities of fluorescence lines with increasing concentration. The E, F, and G groups are almost identical for all three samples examined. The D line does decrease with increasing concentration, but this decrease can be explained as due to self-absorption.

To investigate the origin of the fluorescence lines in more detail, excitation spectra were run on the $CaWO_4$:0.1% Yb sample by using an extremely narrow band-pass interference filter. The filter's transmission was a spike 17 Å wide at 9740 Å with zero transmission to 7500 Å on the high energy side and 1.2 μm on the low side. To obtain high-side blocking through the ultraviolet, a Corning 7-57 infrared-pass-visible-block filter was used with the band-pass filter. The combination was tunable from 9740 to about 8000 Å by changing its angular orientation with respect to the exciting source. This arrangement enabled pumping of any single feature of the absorption spectrum. The spectrum shown in figure 3 was obtained regardless of which part of the absorption spectrum was pumped, including the regions between the main absorption lines and beyond the C line. Moreover, the

fluorescence spectrum, which might be expected to bear some relation to the portion of the absorption spectrum being excited, proved to be relatively independent of the A, B, and C lines. The intensity showed only a small increase when the region between the B and C lines was excited.

The small increase was explained partially by looking at an absorption curve that was taken on the Cary 14 spectrophotometer, a low resolution instrument capable of a wide wavelength range. The three absorption lines A, B, and C were situated on top of continuum that extended from the A line to beyond the C line and peaked in between the B and C lines. Evidently, this continuum is strongly coupled to the A, B, and C lines so that the same fluorescence spectra are produced regardless of where the system is pumped. The intensity follows that of the continuum more closely than that of the absorption lines. The origin of the continuum has not been investigated, but has been conjectured to be the result of a superposition of spectra arising from Yb^{3+} in various lower symmetry sites. That it is related to the ytterbium is fairly certain since it occurs in the same region as the ytterbium absorption lines and there are no other features anywhere else on the absorption spectrum from the ultraviolet absorption edge to the infrared absorption edge. It is possible that this effect is due to the relatively high (1-percent) concentration of Yb^{3+} in the sample. Selective excitation of a lower concentration sample was attempted, but the fluorescence was too weak to give definitive results.

3.1.3 Temperature Effects

Along with polarization and concentration, the effect of temperature was studied. At 26 K the spectral lines broadened somewhat, and at 84 and 300 K some low, broad absorption lines on the low energy side of the A line were observed that were not present at lower

temperatures. Some of these are identified as transitions from the first excited state of the J = 7/2 multiplet. This state is about 200 cm^{-1} above the ground state and has a Boltzmann population ranging from 2 percent (for $CdMoO_4$) to 10 percent (for $BaWO_4$) of the total at 84 K. The lines designated as A' and B' in table 3 were identified from spectra taken at 84 K and refer to transitions from level E_2 to levels E_5 and E_6 of figure 1. The results are consistent with those obtained from fluorescence. In some cases, the D', E', F', and G' lines listed in table 3 also grew in intensity at 84 K.

At 84 K the fluorescence spectrum was poorly resolved, and at 300 K it was unresolved. Measurements were made also at 26 K, but the results were nearly identical to those at 1.9 K.

No significant temperature dependencies were observed for the energies of the different spectral absorption or fluorescence lines. Broadening of the lines appeared to be the major effect of increasing the temperature.

The representations of the lower lying states of Yb^{3+} in $CaWO_4$ and those shown in figure 1 were determined by Jones[11] from crystal-field calculations based on the absorption spectra and the reported fluorescence line wavelengths by Pappalardo and Wood.[10] This identification is consistent with the results obtained here. However, since both the F and G transitions were present in the π spectrum, the reverse assignment with the E_3 level being a $\Gamma_{7,8}$ and the E_4 level being a $\Gamma_{5,6}$ is not precluded by the experimental data. In the accompanying report,[5] it is shown that the assignment given by Jones is in better agreement with crystal-field calculations.

---

[5] *E. A. Brown, Optical Spectra of Yb^{3+} in Crystals with Scheelite Structure, II. Crystal Field Calculations and a Phenomenological Crystal Field Model, Harry Diamond Laboratories HDL-TR-1934 (September 1980).*

[10] *R. Pappalardo and D. L. Wood, J. Mol. Spectrosc., 10 (1963), 81.*

[11] *G. R. Jones, J. Chem. Phys., 47 (1967), 4347.*

3.1.4 Zeeman Effects

The absorption and fluorescence spectra were examined in magnetic fields up to 32 kG. It was found that only the A line could be split sufficiently to obtain accurate g factors. The values obtained with the magnetic field parallel ($g_{\parallel}$) and perpendicular ($g_{\perp}$) to the c axis are given in table 4. The g factors obtained from EPR measurements of the ground state[15] are listed for reference. The g factors for the E_5 level obtained here are in agreement with those reported by Jones.

The axial Zeeman spectrum was examined with a field of 32 kG parallel to the crystal c axis. For this field strength, the A transition is well resolved into three lines in the σ spectrum, but only the central $\sigma\pi$ line appears in the axial spectrum. The result clearly identifies the A line as possessing a magnetic dipole component in

TABLE 4. g FACTORS FOR Yb^{3+} IN CRYSTALS WITH SCHEELITE STRUCTURE

Crystal	Lowest J = 7/2 level*		Lowest J = 5/2 level	
	$g_{\parallel}$	$g_{\perp}$	$g_{\parallel}$	$g_{\perp}$
$CdMoO_4$	1.2393 ± 0.0001	3.917 ± 0.001	-1.31 ± 0.08	1.44 ± 0.11
$CaWO_4$	1.0530 ± 0.0001	3.916 ± 0.001	-1.25 ± 0.15	1.54 ± 0.50
$CaMoO_4$	0.990 ± 0.0002	3.912 ± 0.001	-1.74 ± 0.22	1.44 ± 0.11
$SrWO_4$	0.597 ± 0.0003	3.882 ± 0.002	-0.99 ± 0.30	1.37 ± 0.13
$SrMoO_4$	0.6131 ± 0.0002	3.881 ± 0.001	<-0.51 ± 0.25	1.37 ± 0.06
$PbWO_4$	0.65127 ± 0.00006	3.886 ± 0.001	-1.13 ± 0.07	1.64 ± 0.14
$PbMoO_4$	0.6622 ± 0.0001	3.883 ± 0.001	<-0.50 ± 0.50	1.52 ± 0.13
$BaWO_4$	0.234 ± 0.015	3.882 ± 0.003	-1.07 ± 0.12	1.40 ± 0.11
$LiYF_4$	1.3308 ± 0.0008	3.918 ± 0.003	-1.48 ± 0.07	1.58 ± 0.20

Values from J. P. Sattler and J. Nemarich, Phys. Rev. B, 1 (1970), 4249.

[15] *J. P. Sattler and J. Nemarich, Phys. Rev. B, 1 (1970), 4249.*

agreement with the earlier results by Jones[11] and Kiel and Crane.[13] Figure 4 shows a sample of the Zeeman data recorded for $CaWO_4$:Yb, and figure 5 explains the level splitting scheme for the H∥c case.

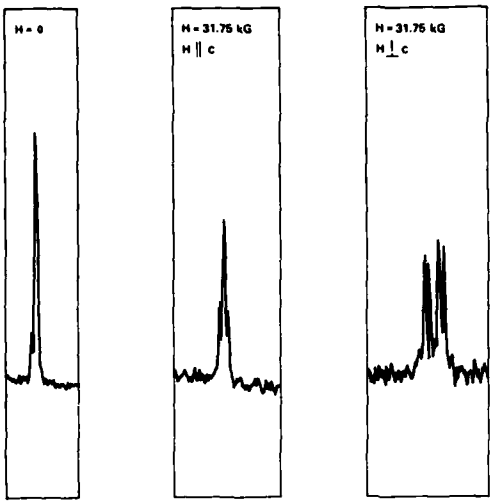

Figure 4. Zeeman splitting of A line in $CaWO_4$:0.1% Yb at 16 K.

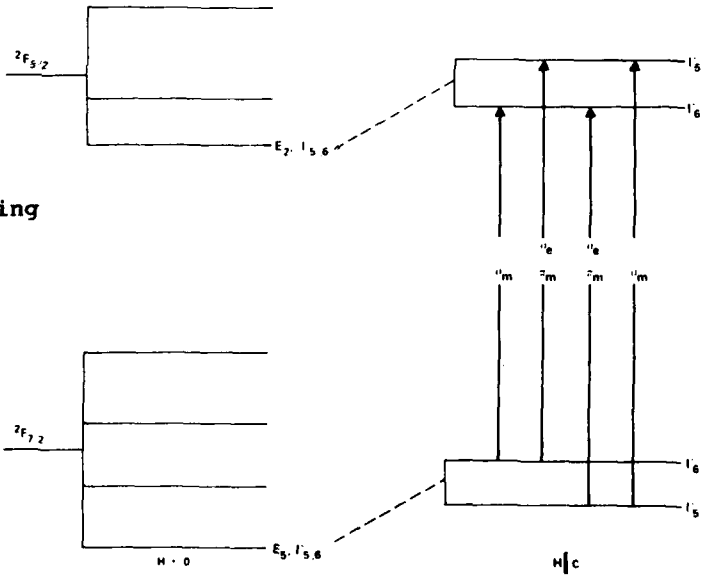

Figure 5. Zeeman splitting and transitions for H∥c axis.

[11] G. R. Jones, J. Chem. Phys., 47 (1967), 4347.
[13] A. Kiel and G. R. Crane, J. Chem. Phys., 48 (1968), 3751

3.2 Spectra of Yb^{3+} in Other Scheelites

In addition to $CaWO_4$:Yb the absorption, fluorescence, and Zeeman spectra were obtained for Yb^{3+} in eight other scheelites as listed in table 1. The procedure used was similar to that described for $CaWO_4$:Yb. Spectra were taken of samples of each scheelite with concentrations of ytterbium ranging from 0.05 atomic percent to several atomic percent and at temperatures ranging from 1.9 to 300 K. Representative results obtained for scheelites investigated in this work are shown elsewhere.[19]

In general, the absorption and fluorescence spectra were similar to those obtained from $CaWO_4$. This similarity was especially so of the seven other tungstate and molybdate scheelites. The main differences from sample to sample aside from the positions of the S_4 transitions as shown in table 3 were the presence or the absence of additional satellite lines on the seven line groups, most of which varied with impurity concentraton. This concentration dependence itself varied from one crystal to another, but the relative intensities of the σ and π spectra of all the scheelites were similar to the intensity observed for $CaWO_4$:Yb. As in $CaWO_4$, the C group was observed only in the σ spectrum for all crystals.

Assignment of an energy for the S_4 transition was difficult when the group consisted of several lines of comparable intensity. The designation of the transition in the figures and the corresponding values listed in table 3 are meant to indicate only the most probable positions of the S_4 transition. These values were arrived at by considering the spectra of Yb^{3+} in several samples of each scheelite and also the relative behavior of the spectra from scheelite to scheelite.

---

[19] *E. A. Brown, Ph.D. Dissertation, New York University (1970).*

The horizontal lines in figures 2 and 3 above certain groups show approximate ranges of energies in which the S_4 transition could be. The corresponding ranges of energies for those crystals not included in the figures were similar to those shown.

All eight tungstate and molybdate scheelites were of the form $A^{2+}(XO_4)^{2-}$, where the Yb^{3+} substituted for the divalent cation, causing a charge discrepancy and necessitating compensation by Na^+ ions. The ninth scheelite investigated had the chemical structure $Y^{3+}(LiF_4)^{3-}$, in which the Yb^{3+} ion now had a trivalent symmetry site to enter, thus eliminating the need for charge compensation and raising the expectation of a simpler, "cleaner" spectrum. To a certain extent, this was indeed so. The A line was exceedingly sharp and narrow (less than one-third the width of the A line in $CaWO_4$) and had no satellites. The B line also was narrow, but had some structure similar to that found in the other crystals. Both A and B were $\sigma\pi$. The C group, again found to be pure σ, consisted of one sharp spike at the low energy end and some lower intensity structure toward the higher energies. The whole group was considerably broader than the C groups in the other samples.

The fluorescence spectrum of $LiYF_4$ was all $\sigma\pi$, as it was in the other scheelites. The D line was narrow with no structure; the F and G lines were diffuse and required compression of the time scale on the chart recorder to determine their locations. The E line was the most unusual feature of this spectrum. It was composed of two sharp, well-separated spikes. Since only one crystal of $LiYF_4:Yb^{3+}$ was available, we could not use concentration effects to aid our selection of the correct line for the E transition. Thus, we had to rely solely on a computer fit (described in a separate report[5]), which indicated the higher energy line of the pair.

[5] E. A. Brown, *Optical Spectra of Yb^{3+} in Crystals with Scheelite Structure, II. Crystal Field Calculations and a Phenomenological Crystal Field Model*, Harry Diamond Laboratories HDL-TR-1934 (September 1980).

The only lines sharp enough for Zeeman splitting to be observed at 32 kG were the A lines of each crystal and the two spikes in the E group of the $LiYF_4:Yb^{3+}$. Based on these measurements, g factors were calculated and used as additional data in the computer fitting program. The values obtained for the g factors of the lowest level in the J = 5/2 manifold (level E_5 in fig. 1) are listed in table 4 with the ground state g factors for each of the nine crystals. The g factors for level E_2 of $LiYF_4:Yb^{3+}$ obtained from splitting the E group in the fluorescence spectrum are $g_{\parallel} = -0.87 \pm 0.17$ and $g_{\perp} = 3.66 \pm 0.30$.

4. DISCUSSION OF S_4 TRANSITIONS

From table 3, some general features of the behavior of the energies of Yb^{3+} in the nine scheelite hosts may be seen. The splitting between the centroids of the J = 7/2 and J = 5/2 manifolds varies little from scheelite to scheelite. The average value of the splittings is 10,160 cm^{-1} with a root mean square (rms) deviation of less than 3 cm^{-1}. The constant value observed agrees with crystal-field theory if the small J-mixing by the crystal field is neglected. In general, the overall splittings of the J = 5/2 and J = 7/2 manifolds decrease in going from the scheelite with the smallest lattice spacing to that with the largest (table 1). For the J = 5/2 manifold, the splitting is a maximum for $CdMoO_4$ (386 cm^{-1}) and a minimum for $LiYF_4$ (259 cm^{-1}). The J = 7/2 manifold has the largest splitting for $CdMoO_4$ and $CaWO_4$ (489 cm^{-1}) and the smallest for $PbMoO_4$ and $BaWO_4$ (406 and 408 cm^{-1}, respectively). These splittings agree with crystal-field theory, which in general predicts a decrease in the splitting of a J manifold with increased lattice spacing.

The EPR results showed that the irreducible representations of the ground state of Yb^{3+} in seven of the eight tungstate and molybdate scheelite hosts are the same ($\Gamma_{5,6}$). Since the absorption transitions from the ground states of these crystals all have the same polarization as for $CaWO_4$, it follows that the representations of their J = 5/2 states also are the same (fig. 1).

Since the EPR results could not definitely assign a representation to the ground state of Yb^{3+} in $BaWO_4$, we must rely on other arguments. As in all the other crystals, the C line appears only in the σ spectrum of $BaWO_4$:Yb, indicating that the ground state and the uppermost state of the J = 5/2 manifold must have the same representation. Because of the smooth increase in the separation between levels E_6 and E_7 with increasing scheelite lattice spacing and the general similarity of the spectra of Yb in all the scheelites, it is unlikely that these two states have crossed in $BaWO_4$. The ground state representation is $\Gamma_{5,6}$ as in the other scheelites, and the ordering of the representations of the J = 5/2 states is as in the other scheelites. Similarly, the experimental data do not preclude a reverse assignment for the representations of E_3 and E_4. However, the representations of the J = 7/2 states are probably the same as for $CaWO_4$.

Nassau[17] and others have shown that many of the satellite lines in the spectra of rare-earth ions in $CaWO_4$ are absent if the crystal is grown with sodium. Since trivalent rare-earth ions substitute for divalent calcium, charge compensating defects or impurities are required to preserve overall charge neutrality. A lattice charge defect near a rare-earth ion lowers the S_4 point symmetry at the ion and causes line broadening or satellite structure in the spectra. Monovalent sodium substitutes for calcium to provide charge compensation and suppresses

[17] *K. Nassau and G. M. Loiacano, J. Phys. Chem Solids, 24 (1963), 1503.*

defect formation. The sodium ion apparently is sufficiently remote from the rare-earth ion to leave it on an undistorted S_4 site. Evidence indicates that this remoteness is the case for rare-earth ions substituted in other tungstate and molybdate scheelites. In $CaWO_4$:Yb, however, sodium compensation does not result in all Yb^{3+} ions being in sites with S_4 symmetry. The EPR spectra of crystals grown with varying amounts of sodium show that the relative number of Yb^{3+} ions in sites with lower symmetry is reduced by adding sodium, but a considerable fraction remains even in crystals grown with a large excess of sodium.[20] Jones[11] shows that the optical absorption spectra of these crystals is simplified somewhat when sodium is added, but that the structures in the B and C groups are mostly unchanged.

In this work, we have examined the spectrum of a crystal grown with a still larger melt ratio of sodium to ytterbium (15 compared with a maximum of 8 used by Jones) and find no differences in the spectra. These findings suggest the possibility of a correlation between at least some of the structures observed in the optical spectra and the persistent low symmetry lines seen in the EPR spectra. This conclusion is further supported by the dependence of the spectra of $CaWO_4$ on ytterbium concentration. Although these effects may be caused in part by a broadening of all spectral lines, they may be due also to a relative increase in the number of Yb^{3+} in sites with lower than S_4 symmetry. The number of these ions should increase proportionately to some higher-than-first power of the ytterbium concentration since the number of charge compensation defects is also a function of the ytterbium concentration.

---

[11] *G. R. Jones, J. Chem. Phys., 47 (1967), 4347.*
[20] *J. Nemarich and W. Viehmann, J. Phys. Chem. Solids, 29 (1968), 57.*

The effect of sodium on the spectra of Yb^{3+} in other scheelites was not investigated to any appreciable extent. Most of the crystals examined were grown with a melt ratio of sodium to ytterbium of four to one. Some crystals grown with a lower ratio were available, and the effect was similar to that observed for $CaWO_4$:Yb.

In spite of the above results, we hesitate to attribute all the structures in the spectra to ytterbium ions in sites with low symmetry until an explanation is found for the polarization of the spectra. A feature common to all the Yb^{3+} spectra observed in this work is the pure σ polarization of the C group. This purity is expected for a transition of an ion in an S_4 site, but not for a transition of an ion in a site with lower than S_4 symmetry. Thus, if low symmetry sites are the explanation of the additional structure in the spectra, the apparent total lack of any π component among the additional structures of the C group is difficult to explain.

The examination of vibronic transitions as a possible explanation for some of the extra structures on the spectra recognized that such transitions could arise from three different mechanisms: (1) coupling of an electronic transition to a zero momentum vibrational mode ($k = 0$) of the lattice, (2) coupling to a $k \neq 0$ mode, and (3) coupling to a local mode, that is, a vibrational mode of one of the heavier impurity ions. Unfortunately, for each of the nine crystals examined, the only published energies available are for $k = 0$ modes obtained from infrared and Raman investigations. These studies[21-27] are for $CaWO_4$, $CaMoO_4$,

[21] J. P. Russell and R. Loudon, Proc. Phys. Soc. (London), 85 (1965), 1025.

[22] S. P. S. Porto and J. F. Scott, Phys. Rev., 157 (1967), 716.

[23] J. F. Scott, J. Chem. Phys., 48 (1968), 874.

[24] A. S. Barker, Jr., Phys. Rev., 135 (1964), A742.

[25] R. K. Khanna, W. S. Brower, B. R. Guscott, and E. R. Lippincott, J. of Research of the National Bureau of Standards, 72A (1968), 81.

[26] J. F. Scott, J. Chem. Phys., 49 (1968), 98.

[27] S. A. Miller, H. E. Rast, and H. H. Caspers, J. Chem. Phys., 52 (1970) 4172.

$SrWO_4$, $SrMoO_4$, $PbWO_4$, $PbMoO_4$, $BaWO_4$, and $LiYF_4$. Thus, the identification of any features of the spectra as $k \neq 0$ vibronics or vibronics stemming from local modes was not possible.

The identification of $k = 0$ vibronics was attempted by observing features on both the absorption and the fluorescence spectra that were higher or lower in energy than one of the S_4 electronic transitions by an amount of energy corresponding to a $k = 0$ lattice mode. Figure 6 shows the absorption and fluorescence spectra for $CaWO_4$:1% Yb at 26 K. The fluorescence spectrum has been reflected about the D line and inverted. This reflection/inversion scheme allows a comparison of differences between various features of the two traces based on the resonant absorption-fluorescent line, A and D, as zero. The scale at the top of the chart indicates the $k = 0$ vibrational energies laid out starting at the A-D line. A similar scale could have been laid out from each of the other S_4 lines, B, C, E, F, and G. The indicated dotted lines connecting points on the two traces link lines of equal energy separation from the A-D line. Those features of either spectrum that match a $k = 0$ mode are candidates for identification as a vibronic transition. Those pairs linked by the dotted lines that match such a mode energy are even stronger candidates by virtue of appearing to indicate a coupling with two of the S_4 transitions. The more of the seven S_4 transitions to which a particular lattice mode appears to have coupled, the stronger the case for the interpretation of those particular spectral lines as vibronics.

The results of this analysis yielded many possible $k = 0$ vibronic transitions within the spectral structure. In fact, in a number of cases, certain $k = 0$ lattice modes appear to have coupled to as many as four and five of the electronic transitions in a single spectrum.

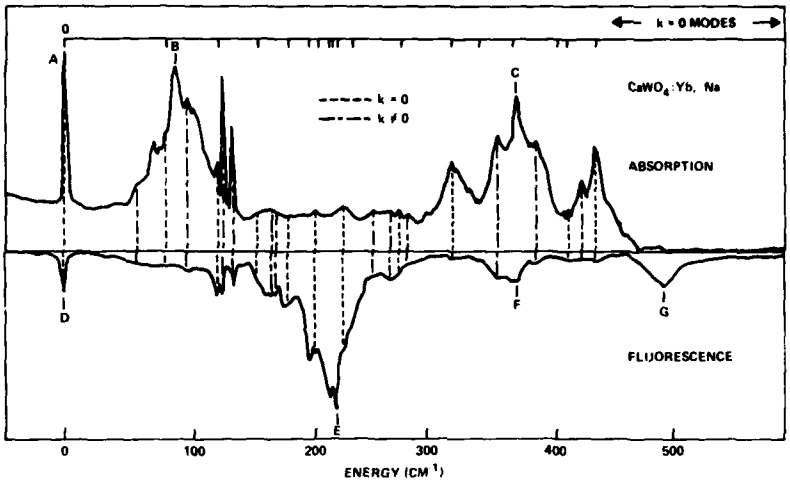

Figure 6. Vibronic structure in spectra of $CaWO_4$:0.1% Yb and 1.5% Na at 26 K.

In addition to analyzing the energies of suspected vibronic transitions, selection rules were calculated and polarization of the spectral lines was considered. The details of the selection rule calculation are given in appendix A. Most of the k = 0 vibronic lines are predicted to be $\sigma\pi$, with a few as pure σ. However, in the region of the C group, no π components are observed. An answer to this problem is suggested by Jones.[11] He proposes a process called selective enhancement of the σ components of vibronics that are nearly degenerate with the C electronic line. Although sufficient data are not available for a fully quantitative evaluation of the matrix elements involved, some qualitative observations can explain this process. The second order matrix elements which contribute to a vibronic transition coupled to the A line are

[11] G. R. Jones, J. Chem. Phys., 47 (1967), 4347.

$$\frac{\langle u_A \eta_1 | \dot{v} | u_n \eta_0 \rangle \langle u_n \eta_0 | P_\varepsilon | u_g \eta_0 \rangle}{(E_A - E_n)} \quad , \tag{1}$$

and

$$\frac{\langle u_A \eta_1 | P_\varepsilon | u_n \eta_1 \rangle \langle u_n \eta_1 | \dot{v} | u_g \eta_0 \rangle}{(E_g - E_n)} \quad . \tag{2}$$

The third order matrix elements which yield a vibronic on the A line in the vicinity of the C line are

$$\frac{\langle u_A \eta_1 | \dot{v} | u_C \eta_0 \rangle \langle u_C \eta_0 | V^{odd} | u_n \eta_0 \rangle \langle u_n \eta_0 | P_\varepsilon | u_g \eta_0 \rangle}{(E_A - E_C)(E_C - E_n)} \quad , \tag{3}$$

$$\frac{\langle u_A \eta_1 | \dot{v} | u_C \eta_0 \rangle \langle u_C \eta_0 | P_\varepsilon | u_n \eta_0 \rangle \langle u_n \eta_0 | V^{odd} | u_g \eta_0 \rangle}{(E_A - E_C)(E_g - E_n)} \quad , \tag{4}$$

and

$$\frac{\langle u_C \eta_0 | \dot{v} | u_A \eta_1 \rangle \langle u_A \eta_1 | P_\varepsilon | u_n \eta_1 \rangle \langle u_n \eta_1 | \dot{v} | u_g \eta_0 \rangle}{(E_A - E_C)(E_g - E_n)} \quad . \tag{5}$$

These five matrix elements are illustrated in figure 7. The operators involved in these equations are P_ε, the electric dipole operator; V^{odd}, the odd crystal-field operator; and $\dot{v}$, the dynamic part of the crystal field. Both P_ε and V^{odd} couple states having opposite parity and the same vibrational mode; $\dot{v}$ couples states in which the vibrational mode changes by ±1 vibrational quantum. The group representation of V^{odd}, as with the rest of the S_4 crystal field, is Γ_1. Therefore, since $|u_C \eta_0\rangle$ and $|u_g \eta_0\rangle$ are $\Gamma_{5,6}$, $|u_n \eta_0\rangle$ in equations (3) and (4) must be $\Gamma_{5,6}$, and P_ε must therefore be a $\Gamma_{3,4}$, that is, a σ_e operator. Thus, equations (3) and (4) are σ-like transitions. Equation (5) involves $\dot{v}$ and may result in σπ transitions. Similarly, equations (1) and (2) are the vibronic terms derived in appendix A and known to contain σπ

transitions. Thus, we would like to be able to say that the sum of equations (3) and (4) is very much greater than the sum of equations (1), (2), and (5), greater to the point that the intensity of any σπ line would be orders of magnitude less than nearby σ lines. The matrix elements equations (3) and (4) are the same as those responsible for the electronic C transition, which has a large transition probability itself, times the factor

$$\frac{\langle u_A \eta_1 | \dot{v} | u_C \eta_0 \rangle}{(E_A - E_C)} \tag{6}$$

If the A vibronic is close to the C line, the denominator $(E_a - E_C)$ is very small and the multiplying factor equation (6) is very large. Thus, equations (3) and (4) are large terms. The terms equations (1), (2), and (5) are all related to the A electronic transition, which has a much smaller transition probability than the C transition. This argument is hardly rigorous, but it at least suggests a possible explanation for the absence of any π component in the C group.

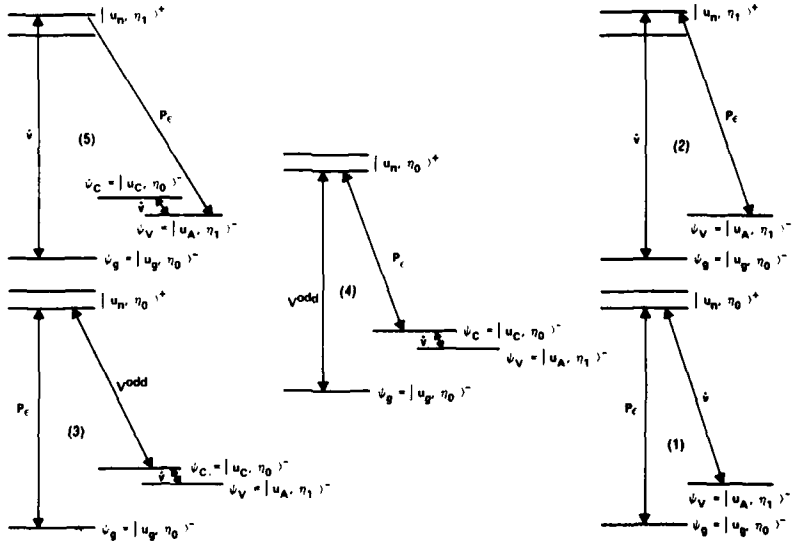

Figure 7. Energy level schemes for selective enhancement of vibronic states.

5. SUMMARY AND CONCLUSIONS

In this experiment, hundreds of spectra were recorded of Yb^{3+} doped into nine different scheelite hosts in varying concentrations. This report has summarized these data. The seven S_4 electronic transitions for each crystal were identified. However, the spectra were rather complex, and thus the identification of the S_4 transitions depended on the identification of the rest of the structure as well. Tentative identifications of most of the spectra were made. Aside from the three absorption and four fluorescence lines from the lowest J = 7/2 and J = 5/2 states, respectively, for each of the nine crystal hosts, transitions from higher levels in each multiplet were seen. This identification was made both by spectral position and by the variation of the intensity of the lines with change in temperature. Other spurious lines on the spectra were identified as originating from Yb ions in low symmetry sites. This conclusion was based on the dependence of these lines with dopant concentration. Finally, many lines were identified as vibronic transitions, some coupling to k = 0 lattice modes whose energies were known and others coupling to $k \neq 0$ modes whose energies were not known, but that appeared to couple to two or more S_4 electronic transitions. The possibility of coupling to local modes was acknowledged, but no such identifications were made.

It is tempting to attribute all this extra structure to low symmetry sites and vibronics, especially the latter since nearly complete sets of lattice modes are found coupled to the A-D line within the regions of the spectral traces, that is, up to about 450 cm^{-1}, as well as a number coupled to B, E, and F lines and even some possibly coupled to the D' line. This attribution may, in fact, be too convenient an explanation since almost all the structure can be explained away as a vibronic of some sort or another. However, it is interesting that although many possible identifications of vibronic transitions are made for the first

18 of the 24 lattice modes of scheelite, not a single line was seen that would correspond to a coupling with the 6 highest energy modes, most of which range from 700 cm^{-1} to 925 cm^{-1}. Coupled with the lack of any of the predicted components in the area of the C group, this lack of correspondence speaks against such identification. The polarization problem also argues against the identification as transitions from low symmetry sites.

On the other hand, both of these problems may be countered by the selective enhancement process described above. Furthermore, Kiel and Crane[13] comment that it can be shown that the necessary shifts in the optical spectra could be caused by changes in the crystal field that would produce only small changes in the state functions. Thus, for the C group, this change would mean that only a small π component would be added to the σ and probably could not be observed.

In summation, the author believes that even though there is a lack of quantitative data concerning vibronics and transitions from low symmetry sites, the qualitative evidence is of such magnitude that the possibility of such phenomena explaining the structure of the subject spectra cannot be ignored. Furthermore, the failure to obey the selection rules that such identifications would seem to demand may be explainable, at least qualitatively, by selective enhancement of the nearby degenerate lines.

---

[13] *A. Kiel and G. R. Crane, J. Chem. Phys., 48 (1968), 3751*

ACKNOWLEDGEMENT

The author thanks the following individuals at the Harry Diamond Laboratories for their many helpful discussions during this work: J. Nemarich, N. Karayianis, C. A. Morrision, J. P. Sattler, and D. E. Wortman. Thanks are offered also to David Chambers for his help in setting up and maintaining the equipment and to R. P. Leavitt for his thoughtful review and comment on the final draft of this report.

LITERATURE CITED

(1) H. J. Van Vleck, J. Phys. Chem. Solids, 27 (1966), 1047.

(2) M. M. Ellis and D. J. Newman, J. Chem. Phys., 47 (1967), 1986.

(3) S. S. Bishton, M. M. Ellis, D. J. Newman, and J. Smith, J. Chem. Phys., 47 (1967), 4133.

(4) R. E. Watson and A. J. Freeman, Phys. Rev., 156 (1967), 251.

(5) E. A. Brown, Optical Spectra of Yb^{3+} in Crystals with Scheelite Structure, II. Crystal Field Calculations and a Phenomenological Crystal Field Model, Harry Diamond Laboratories HDL-TR-1934 (September 1980).

(6) H. E. Swanson, N. T. Gilfrich, and M. I. Cooke, National Bureau of Standards Circular 539, 6 (1956).

(7) H. E. Swanson, N. T. Gilfrich, and M. I. Cooke, National Bureau of Standards Circular 539, 7 (1957).

(8) A. Zalkin and D. H. Templeton, J. Chem. Phys., 40 (1964), 501.

(9) J. Leciejewicz, Z. Kristallogr., 121 (1965), 158.

(10) R. Pappalardo and D. L. Wood, J. Mol. Spectrosc., 10 (1963), 81.

(11) G. R. Jones, J. Chem. Phys., 47 (1967), 4347.

(12) G. F. Koster, J. O. Dimmock, R. G. Wheeler, and H. Statz, Properties of the Thirty-Two Point Groups, Massachusetts Institute of Technology Press, Cambridge, MA (1963).

(13) A. Kiel and G. R. Crane, J. Chem. Phys., 48 (1968), 3751.

(14) U. Ranon and V. Volterra, Phys. Rev., 134 (1964), A1483.

(15) J. P. Sattler and J. Nemarich, Phys. Rev. B, 1 (1970), 4249.

(16) R. M. Curnutt, Czochralski Growth of Tungstate and Molybdate Scheelites, Harry Diamond Laboratories HDL-TM-70-8 (July 1970).

(17) K. Nassau and G. M. Loiacano, J. Phys. Chem. Solids, 24 (1963), 1503.

(18) E. V. Sayre, K. M. Sancier, and S. Freed, J. Chem. Phys., 23 (1955), 2060.

(19) E. A. Brown, Ph.D. Dissertation, New York University (1970).

(20) J. Nemarich and W. Viehmann, J. Phys. Chem. Solids, 29 (1968), 57.

(21) J. P. Russell and R. Loudon, Proc. Phys. Soc. (London), 85 (1965), 1025.

(22) S. P. S. Porto and J. F. Scott, Phys. Rev., 157 (1967), 716.

(23) J. F. Scott, J. Chem. Phys., 48 (1968), 874.

(24) A. S. Barker, Jr., Phys. Rev., 135 (1964), A742.

(25) R. K. Khanna, W. S. Brower, B. R. Guscott, and E. R. Lippincott, J. of Research of the National Bureau of Standards, 72A (1968), 81.

(26) J. F. Scott, J. Chem. Phys., 49 (1968), 98.

(27) S. A. Miller, H. E. Rast, and H. H. Caspers, J. Chem. Phys., 52 (1970) 4172.

APPENDIX A.--CALCULATION OF THE SELECTION RULES FOR VIBRONIC TRANSITIONS

The tentative identification of some of the spurious lines in a spectrum as vibronic transitions required an investigation of their polarization properties with the attendant calculation of their selection rules. Calculation of vibronic selection rules is a moderately complex procedure that must be carried out anew for each space group with which one is concerned. To provide a summarized reference of the procedure as well as the results for the space group of the scheelite lattice, the calculation is reproduced here. It is based mainly on the works of Satten,[1] Smith and Sorokin,[2] and Cohen and Moos.[3]

We begin by considering an energy level scheme (fig. A-1) showing two electronic levels of an ion, a ground state and the nth excited state. The vibrational states of the lattice in which the ion is imbedded are superimposed on each electronic state, indicating the coupled (vibronic) states of the ion-lattice system. Also shown are two examples of vibronic transitions. The transition "A" represents an absorption from the ground state consisting of the lowest electronic state of the ion and the zero phonon state of the lattice to the nth excited electronic state coupled to the first excited vibrational state. The transition "B" is a similar fluorescent vibronic.

---

[1] *R. A. Satten, J. Chem. Phys., 40 (1964), 1200.*

[2] *W. V. Smith and P. P. Sorokin, The Laser, McGraw-Hill Book Co., New York (1966).*

[3] *E. Cohen and H. W. Moos, Phys. Rev., 161 (1967), 258.*

APPENDIX A

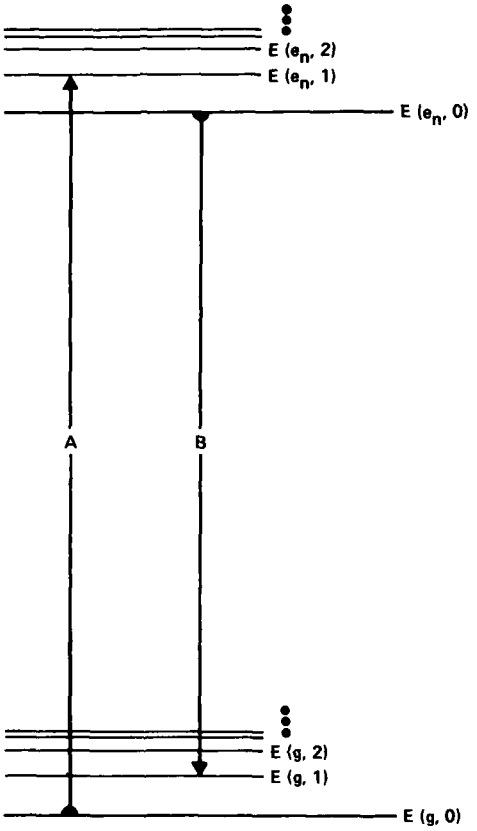

Figure A-1. Typical vibronic transition.

The crystal-field energy of the electrons in unfilled shells of a central ion in a vibrating complex can be written as

$$V_c = -e \sum_{i,j} \left[\frac{e_i}{\left|\vec{R}_i - \vec{r}_j\right|} + \frac{\vec{p}_i\left(\vec{R}_i - \vec{r}_j\right)}{\left|\vec{R}_i - \vec{r}_j\right|^3} + \cdots \right] \qquad \text{(A-1)}$$

$$= \sum_{i,j} v_i^{(j)}\left(\vec{R}_i - \vec{r}_j\right) \quad ,$$

which is just the general multipole expansion of electrostatic energy. Here, $\vec{R}_i$ locates the ith ion in the complex, and $\vec{r}_j$ locates the jth electron in the unfilled shell of that ion. The effective charge and the dipole moment of the ith ion are given by e_i and p_i, respectively. The difference between the potential energy, V_c, in a displaced position and in the equilibrium position is the vibronic interaction. It is given to first order by the expression

$$\mathcal{H} = \left(V_{c_{disp}} - V_{c_{equil}}\right) = \sum_i \left(\Delta X_i \frac{\partial}{\partial X_i} + \Delta Y_i \frac{\partial}{\partial Y_i} + \Delta Z_i \frac{\partial}{\partial Z_i}\right) V_c \quad . \tag{A-2}$$

Since

$$\frac{\partial V_c}{\partial X_i} = \frac{\partial \sum_j V_i^{(j)}}{\partial X_i} = -\sum_j \frac{\partial V_i^{(j)}}{\partial x_j} \quad , \tag{A-3}$$

we have

$$\mathcal{H} = -\sum_{i,j} \left(\Delta X_i \frac{\partial}{\partial x_j} + \Delta Y_i \frac{\partial}{\partial y_j} + \Delta Z_i \frac{\partial}{\partial z_j}\right) V_i^{(j)} \quad . \tag{A-4}$$

The relationship between the displacements and the normal coordinates is

$$\Delta X_i = \sum_k S_{ix,k} Q_k \quad , \tag{A-5}$$

where the sum is over the normal coordinates. Putting this into the expression for $\mathcal{H}$,

APPENDIX A

$$\mathcal{H} = -\sum_k Q_k \sum_{i,j} \left(S_{ix,k} \frac{\partial v_i^{(j)}}{\partial x_j} + S_{iy,k} \frac{\partial v_i^{(j)}}{\partial y_j} + S_{iz,k} \frac{\partial v_i^{(j)}}{\partial z_j} \right)$$

$$= -\sum_k \sum_j Q_k V_k^{(j)} \qquad \text{(A-6)}$$

The derivatives in the expression for $V_k^{(j)}$ are all with respect to the equilibrium position of the ions in the complex. This expression for $\mathcal{H}$ defines operators $V_k^{(j)}$, which represents the dynamic part of the crystal field and which operates only on the ion electronic states, and Q_k, which operates only on the vibrational (phonon) states.

The desired matrix elements are those that connect, for example, $E(g,0)$ and $E(e_n,1)$ in figure A-1. The wave function for some generalized excited state such as $E(e_n,1)$ may be written as

$$\psi_e \approx |u_e \eta_1(Q_r)\rangle - \sum_n \frac{\langle u_n \eta_0(Q_r) | \mathcal{H} | u_e \eta_1(Q_r)\rangle}{(E_n - E_e)} |u_n \eta_0(Q_r)\rangle$$

$$- \sum_n \frac{\langle u_n \eta_2(Q_r) | \mathcal{H} | u_e \eta_1(Q_r)\rangle}{(E_n - E_e)} |u_n \eta_2(Q_r) \qquad \text{(A-7)}$$

where the η's are the three lowest energy vibrational wave functions of the normal mode $Q(r)$, and u_e and u_n are pure electronic wave functions. The summation is over all electronic states. ψ_e can be interpreted as the wave function of the level $E(e_1,1)$ with two correction terms for all other states of one more or one less quantum of vibrational energy, that is, $E(e_n,0)$ and $E(e_n,2)$, which are mixed into $E(e_1,1)$ by $\mathcal{H}$. A similar expression can be written for the ground state, $E(g,0)$:

$$\psi_g = |u_g \eta_0(Q_r)\rangle - \sum_n \frac{\langle u_n \eta_1(Q_r)|\mathcal{H}|u_g \eta_0(Q_r)\rangle}{(E_n - E_g)} |u_n \eta_1(Q_r)\rangle \cdot \quad \text{(A-8)}$$

Here, there is only one correction term since there is no vibrational state lower than E(g,0) to mix in.

To form the matrix elements with the electric dipole operator, we consider a general component of

$$\vec{P} = \sum_j e\vec{r}_j \quad \text{(A-9)}$$

of the form

$$P_\varepsilon = \sum_j p^{(j)} \quad . \quad \text{(A-10)}$$

The details of the matrix element calculation can be found elsewhere.[2-4] The result of such a calculation is

$$\langle \psi_e | P_\varepsilon | \psi_g \rangle = \sum_n \left(\frac{\hbar}{4\pi\nu_r}\right)^{1/2} \left(\frac{\langle u_n | \sum_j v_r^{(j)} | u_g \rangle \langle u_e | \sum_j p^{(j)} | u_n \rangle}{(E_n - E_g)} \right.$$

---

[2] *W. V. Smith and P. P. Sorokin, The Laser, McGraw-Hill Book Co., New York (1966).*

[3] *E. Cohen and H. W. Moos, Phys. Rev., 161 (1967), 258.*

[4] *E. Cohen, Ph.D. Dissertation, The Johns Hopkins University (1967).*

APPENDIX A

$$+ \frac{\langle u_n | \sum_j v_r^{(j)} | u_e \rangle \langle u_g | \sum_j p^{(j)} | u_n \rangle}{(E_n - E_e)} \Bigg) . \qquad \text{(A-11)}$$

To obtain the selection rules for transitions between ψ_e and ψ_g, the group properties of ψ_e, ψ_g, and P_ε can be employed. ψ_g consists of a ground electronic state with irreducible representation Γ_a and the ground state of the phonons, which transforms like the identity. Thus, $\Gamma_g = \Gamma_a$. ψ_e consists of the excited electronic state having the representation Γ_b and an excited phonon state, which transforms like Γ, the representation of the phonon site group, that is, the symmetry group of the point in the Brillouin zone from which the phonon originates. Thus $\Gamma_e = \Gamma \times \Gamma_b$. The components of the operator transform as Γ_i according to the scheme of the basis functions for the S_4 single group. For electric dipole operator with $\vec{E} \| z$, that is π_e, Γ_i is Γ_2; for $E \perp z$, that is, σ_e, Γ_i is $\Gamma_{3,4}$. For the magnetic dipole, Γ_i is Γ_1 for σ_m and $\Gamma_{3,4}$ for π_m. Thus, the following selection rule is obtained. For a matrix element formed with operator P that transforms as the irreducible representation Γ_i, $\langle \psi_e | P | \psi_g \rangle = 0$ unless Γ_i is contained in the product $\Gamma_a \times \Gamma \times \Gamma_b$. The irreducible representations of the electronic states, Γ_a and Γ_b, are shown in figure 1. However, the irreducible representation of the phonon state is yet to be determined. To determine it, we consider the space group properties of the scheelite lattice, which is a tetragonal, body-centered system belonging to the space group $C_{4h}^6(I4_1/a)$. It is necessary to express Γ in terms of the irreducible representations of the rare-earth point group, S_4.

APPENDIX A

The density of states of lattice modes is given by[3,4]

$$G(\omega^2) = \frac{V_o}{(2\pi)^3 r} \int_{s(\omega^2)} \frac{ds}{|\nabla_k \omega^2|} , \qquad \text{(A-12)}$$

where V_o is the unit cell volume, r is the number of atoms in the unit cell, and $s(\omega^2)$ is the surface of constant $\omega^2(k)$. The properties of this function are discussed by Weinrich[5] and by Cohen.[3,4] For our purposes, it is sufficient to note that there are maxima in $G(\omega^2)$ whenever $\nabla_k \omega^2 \to 0$, which condition can occur at a point of high symmetry in the Brillouin zone, that is, a point at which the group for $\vec{k}$ contains more than just the identity operator. Thus, at these points there is a clumping of a large number of modes of approximately the same energy and symmetry. For this reason, only these high symmetry points are considered. Figure A-2 shows the Brillouin zone for a tetragonal, body-centered lattice with the high symmetry points indicated. Only k = 0 phonons, that is, those originating at the point Γ in the Brillouin zone, have had their energies tabulated. Thus, this calculation is concerned only with those phonons. The entire calculation for all the high symmetry points can be found elsewhere.[6]

---

[3] *E. Cohen and H. W. Moos, Phys. Rev., 161 (1967), 258.*

[4] *E. Cohen, Ph.D. Dissertation, The Johns Hopkins University (1967).*

[5] *G. Weinreich, Solids: Elementary Theory for Advanced Students, John Wiley and Sons, Inc., New York (1965), 73 ff.*

[6] *E. A. Brown, Ph.D. Dissertation, New York University (1970).*

APPENDIX A

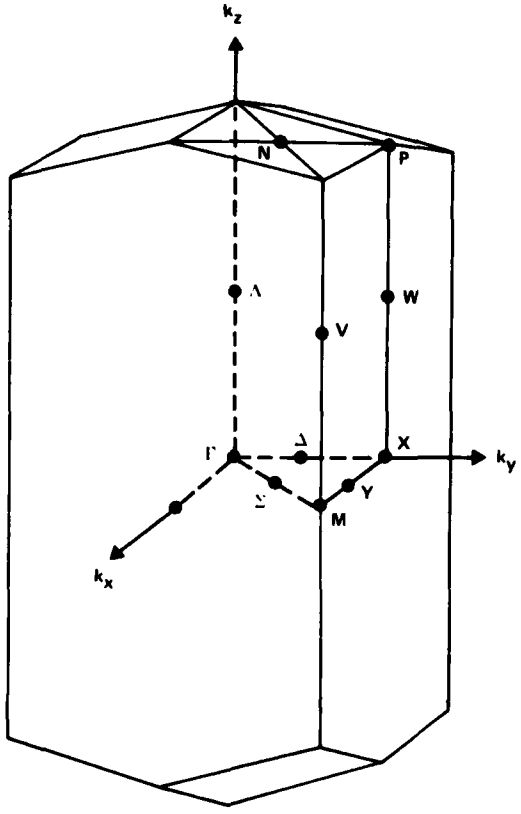

Figure A-2. Brillouin zone for tetragonal, body-centered lattice.

The method used in resolving the representation of the phonon site group, Γ, into representations in S_4 symmetry, the symmetry of the rare-earth site, is from Satten.[1] Basically, this method involves considering the character tables for the site group of each high symmetry point in the Brillouin zone, observing which elements the phonon site group has in common with the S_4 point group, and then decomposing each representation in each phonon site group into a sum of S_4 irreducible representations. The character tables of each high symmetry point are tabulated by Miller and Love.[7] Table A-1 is the character table for point Γ.

[1] *R. A. Satten, J. Chem. Phys., 40 (1964), 1200.*

[7] *S. C. Miller and W. F. Love, Irreducible Representations of Space Groups, Pruett Press, Boulder, CO (1967).*

APPENDIX A

TABLE A-1. CHARACTER TABLES FOR HIGH SYMMETRY POINT Γ IN BRILLOUIN ZONE OF SCHEELITE (C_{4h}^6)

	E	C_2	σ_h	I	C_4	C_4^{-1}	S_4	S_4^{-1}
Γ_1^+	1	1	1	1	1	1	1	1
Γ_2^+	1	1	1	1	-1	-1	-1	-1
Γ_3^+	1	-1	-1	1	i	-i	-i	i
Γ_4^+	1	-1	-1	1	-i	i	i	-i
Γ_1^-	1	1	-1	-1	1	1	-1	-1
Γ_2^-	1	1	-1	-1	-1	-1	1	1
Γ_3^-	1	-1	1	-1	i	-i	i	-i
Γ_4^-	1	-1	1	-1	-i	i	-i	i

We begin by defining the "star" of the vector $\vec{k}$ as the set of q distinct vectors, $\vec{k}_i = \alpha_i \vec{k}$, i = 1, . . ., q, into which $\vec{k}$ is transformed under the operations of the crystal point group. Since the space group representation includes all vectors of the star of $\vec{k}$ at each point in the Brillouin zone, it is necessary to multiply the characters of the site group at each point in the Brillouin zone by the number of vectors in the star of $\vec{k}$ for that point. The number of vectors in the star of $\vec{k}$ for a particular point is equal to the order of the crystal point group--in this case, C_{4h}--divided by the order of the site point group. The order of a group is given by the number of elements in a group. For symmetry point Γ, the phonon site group is C_{4h}, which has order 8. There is one vector in the star of $\vec{k}$ for point Γ. To obtain the space group irreducible representation characters, the site group character table (table A-1) is multiplied by the number of vectors in the star of the respective $\vec{k}$. These results are listed in table A-2. We are concerned only with those elements that are common to the rare-earth ion site group, S_4. Each representation of each point group of the k vector is examined to see how it can be reduced into a linear combination of representations of its S_4 point group.

APPENDIX A

TABLE A-2. S_4 COMPONENT OF C_{4h}^6 SPACE GROUP CHARACTER TABLE (Γ ONLY)

	E	C_2	S_4	S_4^{-1}
Γ_1^+	1	1	1	1
Γ_2^+	1	1	-1	-1
Γ_3^+	1	-1	-i	i
Γ_4^+	1	-1	i	-i
Γ_1^-	1	1	-1	-1
Γ_2^-	1	1	1	1
Γ_3^-	1	-1	i	-i
Γ_4^-	1	-1	-i	i

As an example, we take the representation Γ_3^-. By comparison with the S_4 character table,[8] we see that, as an example, the Γ_3^- representation of the Γ point of the Brillouin zone is equivalent to a Γ_4 representation of the S_4 point group. By such a series of comparisons, the full reduction table for all representations of the C_{4h}^6 space group to the S_4 point group can be obtained. Although only the Γ point is of interest, the whole reduction table is given for reference as table A-3. Now it is possible to complete the determination of the vibronic selection rules. The irreducible representation of the phonon state, Γ, can now be found to be some linear combination of irreducible representations of S_4.

[8] *G. F. Koster, J. O. Dimmock, R. G. Wheeler, and H. Statz, Properties of the Thirty-Two Point Groups, Massachusetts Institute of Technology Press, Cambridge, MA (1963).*

TABLE A-3. SPACE GROUP REDUCTION COEFFICIENTS: $C_{4h}^6 \rightarrow S_4$

	Γ_1	Γ_2	Γ_3	Γ_4
Γ_1^+	1			
Γ_2^+		1		
Γ_3^+			1	
Γ_4^+				1
Γ_1^-		1		
Γ_2^-	1			
Γ_3^-				1
Γ_4^-			1	
Λ_1	1	1		
Λ_2	1	1		
Λ_3			1	1
Λ_4			1	1
Σ_1	1	1	1	1
Σ_2	1	1	1	1
Δ_1	1	1	1	1
Δ_2	1	1	1	1

	Γ_1	Γ_2	Γ_3	Γ_4
M_1	1	1		
M_2			1	1
P_1	2			
P_2		2		
P_3				2
P_4			2	
V_1	1	1		
V_2	1	1		
V_3			1	1
V_4			1	1
X_1	1	1	1	1
W_1	2	2		
W_2			2	2
N_1^+	1	1	1	1
N_1^-	1	1	1	1
Y_1	1	1	1	1
Y_2	1	1	1	1

As an example, consider the representation Γ_3^-:

$$\Gamma_3^- = \Gamma_4 \qquad \text{(A-13)}$$

For a transition of the type $\Gamma_5 \rightarrow \Gamma_6$, we have

APPENDIX A

$$\Gamma_5^* \times \Gamma_3^- \times \Gamma_6 = \Gamma_6 \times \Gamma_4 \times \Gamma_6$$

$$= \Gamma_6 \times \Gamma_5 \qquad \text{(A-14)}$$

$$= \Gamma_1 \quad .$$

This indicates an allowed vibronic transition by the operator σ_m. The vibronic selection rules for point Γ are summarized in table A-4.

TABLE A-4. SELECTION RULES FOR VIBRONIC TRANSITIONS COUPLING k = 0 MODES

	Transitions from Γ_5				Γ_6				Γ_7				Γ_8			
Transitions to	Γ_5	Γ_6	Γ_7	Γ_8	Γ_5	Γ_6	Γ_7	Γ_8	Γ_5	Γ_6	Γ_7	Γ_8	Γ_5	Γ_6	Γ_7	Γ_8
Γ_1^+	π_m	σ	π_e	σ	σ	π_m	σ	π_e	π_e	σ	π_m	σ	σ	π_e	σ	π_m
Γ_2^+	π_e	σ	π_m	σ	σ	π_e	σ	π_m	π_m	σ	π_e	σ	σ	π_m	σ	π_e
Γ_3^+	σ	π_e	σ	π_m	π_e	σ	π_m	σ	σ	π_m	σ	π_e	π_m	σ	π_e	σ
Γ_4^+	σ	π_m	σ	π_e	π_m	σ	π_e	σ	σ	π_e	σ	π_m	π_e	σ	π_m	σ
Γ_1^-	π_e	σ	π_m	σ	σ	π_e	σ	π_m	π_e	σ	π_m	σ	σ	π_e	σ	π_m
Γ_2^-	π_m	σ	π_e	σ	σ	π_m	σ	π_e	π_m	σ	π_e	σ	σ	π_m	σ	π_e
Γ_3^-	σ	π_m	σ	π_e	π_m	σ	π_e	σ	σ	π_e	σ	π_m	π_e	σ	π_m	σ
Γ_4^-	σ	π_e	σ	π_m	π_e	σ	π_m	σ	σ	π_m	σ	π_e	π_m	σ	π_e	σ

APPENDIX A

LITERATURE CITED

(1) R. A. Satten, J. Chem. Phys., 40 (1964), 1200.

(2) W. V. Smith and P. P. Sorokin, The Laser, McGraw-Hill Book Co., New York (1966).

(3) E. Cohen and H. W. Moos, Phys. Rev., 161 (1967), 258.

(4) E. Cohen, Ph.D. Dissertation, The Johns Hopkins University (1967).

(5) G. Weinreich, Solids: Elementary Theory for Advanced Students, John Wiley and Sons, Inc., New York (1965), 73 ff.

(6) E. A. Brown, Ph.D. Dissertation, New York University (1970).

(7) S. C. Miller and W. F. Love, Irreducible Representations of Space Groups, Pruett Press, Boulder, CO (1967).

(8) G. F. Koster, J. O. Dimmock, R. G. Wheeler, and H. Statz, Properties of the Thirty-Two Point Groups, Massachusetts Institute of Technology Press, Cambridge, MA (1963).

DISTRIBUTION

DEFENSE DOCUMENTATION CENTER
CAMERON STATION, BUILDING 5
ATTN DDC-TCA (12 COPIES)
ALEXANDRIA, VA 22314

COMMANDER
US ARMY RSCH & STD GP (EUR)
ATTN CHIEF, PHYSICS & MATH BRANCH
BOX 65
FPO NEW YORK 09510

COMMANDER
US ARMY MATERIEL DEVELOPMENT & READINESS COMMAND
ATTN DRCDE, DIR FOR DEV & ENG
ATTN DRCDMD-ST
ATTN DRCLDC (JAMES BENDER)
5001 EISENHOWER AVENUE
ALEXANDRIA, VA 22333

COMMANDER
US ARMY ARMAMENT MATERIEL READINESS COMMAND
ATTN DRSAR-ASF, FUZE & MUNITIONS SPT DIV
ATTN DRSAR-LEP-L, TECHNICAL LIBRARY
ROCK ISLAND ARSENAL
ROCK ISLAND, IL 61299

COMMANDER
US ARMY MISSILE & MUNITIONS CENTER & SCHOOL
ATTN ATSK-CTD-F
REDSTONE ARSENAL, AL 35809

DIRECTOR
US ARMY MATERIEL SYSTEMS ANALYSIS ACTIVITY
ATTN DRXSY-MP
ABERDEEN PROVING GROUND, MD 21005

TELEDYNE BROWN ENGINEERING
CUMMINGS RESEARCH PARK
ATTN DR. MELVIN L. PRICE, MS-44
HUNTSVILLE, AL 35807

ENGINEERING SOCIETIES LIBRARY
ATTN ACQUISITIONS DEPARTMENT
345 EAST 47TH STREET
NEW YORK, NY 10017

US ARMY ELECTRONICS TECHNOLOGY
& DEVICES LABORATORY
ATTN DELET-DD
ATTN DELET-MJ (DR. HAROLD JACOBS)
FORT MONMOUTH, NH 07703

DEPARTMENT OF DEFENSE
OUSDR&E
ATTN DR. GEORGE G. GOMOTA
WASHINGTON, DC 20301

DIRECTOR
DEFENSE ADVANCED RESEARCH PROJECTS AGENCY
ARCHITECT BLDG
ATTN DEPUTY DIRECTOR FOR RESEARCH
ATTN DR. DOUGLAS H. TANIMOTO
1400 WILSON BLVD
ARLINGTON, VA 22209

DIRECTOR
DEFENSE NUCLEAR AGENCY
ATTN APTL, TECH LIBRARY
ATTN DR. EDWARD CONRAD
ATTN DR. ROBERT OSWALD
WASHINGON, DC 20305

UNDER SECRETARY OF DEFENSE FOR RES AND
ENGINEERING
ATTN TECHNICAL LIBRARY (3C128)
WASHINGTON, DC 20301

OFFICE, CHIEF OF RESEARCH,
DEVELOPMENT, & ACQUISITION
DEPARTMENT OF THE ARMY
ATTN DAMA-AR, DR. M. E. LASSER
ATTN DAMA-ARZ-D, DR. F. VERDERAME
WASHINGTON, DC 20310

COMMANDER
US ARMY RESEARCH OFFICE (DURHAM)
ATTN DR. ROBERT LONTZ (2 COPIES)
PO BOX 12211
RESEARCH TRIANGLE PARK, NC 27709

COMMANDER
ARMY MATERIALS & MECHANICS RESEARCH
CENTER
ATTN DRXMR-TL, TECH LIBRARY BR
WATERTOWN, MA 02172

COMMANDER
NATICK LABORATORIES
ATTN DRXRES-RTL, TECH LIBRARY
NATICK, MA 01762

COMMANDER
USA FOREIGN SCIENCE & TECHNOLOGY CENTER
ATTN DRXST-BS, BASIC SCIENCE DIV
FEDERAL OFFICE BUILDING
220 7TH STREET NE
CHARLOTTESVILLE, VA 22901

DIRECTOR
US ARMY BALLISTICS RESEARCH LABORATORY
ATTN DRXBR, DIRECTOR, R. EICHELBERGER
ATTN DRXBR-TB, FRANK J. ALLEN
ATTN DRXBR, TECH LIBRARY
ATTN DRDAR-TSB-S (STINFO)
ABERDEEN PROVING GROUND, MD 21005

DISTRIBUTION (Cont'd)

DIRECTOR
ELECTRONIC WARFARE LABORATORY
ATTN TECHNICAL LIBRARY
ATTN J. CHARLTON
ATTN DR. HIESLMAIR
ATTN J. STROZYK
ATTN DR. E. J. TEBO
FT MONMOUTH, NJ 07703

DIRECTOR
NIGHT VISION & ELECTRO-OPTICS LABORATORY
ATTN TECHNICAL LIBRARY
ATTN R. BUSER
ATTN G. JONES
FT BELVOIR, VA 22060

COMMANDER
ATMOSPHERIC SCIENCES LABORATORY
ATTN TECHNICAL LIBRARY
WHITE SANDS MISSILE RANGE, NM 88002

DIRECTOR
DEFENSE COMMUNICATIONS ENGINEERING CENTER
ATTN PETER A, VENA
1860 WIEHLE AVE
RESTON, VA 22090

COMMANDER
US ARMY MISSILE COMMAND
ATTN DRDMI-TB, REDSTONE SCI INFO CENTER
ATTN DRCPM-HEL, DR. W. B. JENNINGS
ATTN DR. J. P. HALLOWES
ATTN T. HONEYCUTT
REDSTONE ARSENAL, AL 35809

COMMANDER
EDGEWOOD ARSENAL
ATTN SAREA-TS-L, TECH LIBRARY
EDGEWOOD ARSENAL, MD 21010

COMMANDER
US ARMY ARMAMENT RES & DEV COMMAND
ATTN DRDAR-TSS, STINFO DIV
DOVER, NJ 07801

COMMANDER
US ARMY TEST & EVALUATION COMMAND
ATTN TECH LIBRARY
ABERDEEN PROVING GROUND, MD 21005

COMMANDER
US ARMY ABERDEEN PROVING GROUND
ATTN STEAP-TL, TECH LIBRARY, BLDG 305
ABERDEEN PROVING GROUND, MD 21005

COMMANDER
ATTN DRSEL-WL-MS, ROBERT NELSON
WHITE SANDS MISSILE RANGE, NM 88002

COMMANDER
GENERAL THOMAS J. RODMAN LABORATORY
ROCK ISLAND ARSENAL
ATTN SWERR-PL, TECH LIBRARY
ROCK ISLAND, IL 61201

COMMANDER
US ARMY CHEMICAL CENTER & SCHOOL
FORT MCCLELLAN, AL 36201

COMMANDER
NAVAL OCEAN SYSTEMS CENTER
ATTN TECH LIBRARY
SAN DIEGO, CA 92152

COMMANDER
NAVAL SURFACE WEAPONS CENTER
ATTN WX-40, TECHNICAL LIBRARY
WHITE OAK, MD 20910

DIRECTOR
NAVAL RESEARCH LABORATORY
ATTN CODE 2620, TECH LIBRARY BR
ATTN CODE 5554, DR. LEON ESTEROWITZ
ATTN CODE 5554, DR. S. BARTOLI
ATTN CODE 5554, R. E. ALLEN
WASHINGTON, DC 20390

COMMANDER
NAVAL WEAPONS CENTER
ATTN CODE 753, LIBRARY DIV
CHINA LAKE, CA 93555

OFFICE OF NAVAL RESEARCH
ATTN DR. V. O. NICOLAI
ARLINGTON, VA 22217

COMMANDER
AF ELECTRONICS SYSTEMS DIV
ATTN TECH LIBRARY
L. G. HANSCOM AFB, MA 01730

DEPARTMENT OF COMMERCE
NATIONAL BUREAU OF STANDARDS
ATTN LIBRARY
ATTN DR. W. BROWNER
ATTN H. S. PARKER
WASHINGTON, DC 20234

DIRECTOR
LAWRENCE RADIATION LABORATORY
ATTN DR. MARVIN J. WEBER
ATTN DR. HELMUT A. KOEHLER
LIVERMORE, CA 94550

NASA GODDARD SPACE FLIGHT CENTER
ATTN CODE 252, DOC SECT, LIBRARY
GREENBELT, MD 20771

NASA HEADQUARTERS
ATTN RTE-G (DR. M. SOKOLOSKI)
WASHINGTON, DC 20546

NATIONAL OCEANIC & ATMOSPHERIC ADM
ENVIRONMENTAL RESEARCH LABORATORIES
ATTN LIBRARY, R-51, TECH REPORTS
BOULDER, CO 80302

DIRECTOR
ADVISORY GROUP ON ELECTRON DEVICES
ATTN SECTRY, WORKING GROUP D
201 VARICK STREET
NEW YORK, NY 10013

THE AEROSPACE CORPORATION
THE IVAN A. GETTING LABORATORY
ATTN DR. DEAN T. HODGES
PO BOX 92957
LOS ANGELES, CA 90009

HONEYWELL CORPORATE RESEARCH CENTER
ATTN DR. PAUL W. KRUSE
10701 LYNDALE AVENUE SOUTH
BLOOMINGTON, MN 55420

BOOZ-ALLEN & HAMILTON
ATTN BRUCE M. FONOROFF
ATTN HARRY GIESKE
4330 EAST-WEST HIGHWAY
BETHESDA, MD 20014

CARNEGIE MELLON UNIVERSITY
SCHENLEY PARK
ATTN PHYSICS & EE
DR. J. O. ARTMAN
PITTSBURGH, PA 15213

UNIVERSITY OF MICHIGAN
COLLEGE OF ENGINEERING NORTH CAMPUS
DEPARTMENT OF NUCLEAR ENGINEERING
ATTN DR. CHIHIRO KIKUCHI
ANN ARBOR, MI 48104

CRYSTAL PHYSICS LABORATORY
MASSACHUSETTS INSTITUTE OF TECHNOLOGY
ATTN DR. A. LINZ
ATTN DR. H. P. JENSSEN
CAMBRIDGE, MA 02139

CENTER FOR LASER STUDIES
UNIVERSITY OF SOUTHERN CALIFORNIA
ATTN DR. L. G. DE SHAZER
LOS ANGELES, CA 90007

JOHNS HOPKINS UNIVERSITY
PHYSICS DEPARTMENT
ATTN PROF B. R. JUDD
BALTIMORE, MD 21218

ARGONNE NATIONAL LABORATORY
ATTN DR. W. T. CARNALL
9700 SOUTH CASS AVENUE
ARGONNE, IL 60439

MONTANA STATE UNIVERSITY
PHYSICS DEPT
ATTN PROF RUFUS L. CONE
BOZEMAN, MT 59715

NORTH DAKOTA STATE UNIVERSITY
PYSICS DEPT
ATTN PROF J. GRUBER
FARGO, ND 58102

RARE-EARTH INFORMATION CENTER
ENERGY AND MINERAL RESOURCES RESEARCH INSTITUTE
ATTN DR. KARL GSCHNEIDNER, JR.
IOWA STATE UNIVERSITY
AMES, IA 50011

US ARMY ELECTRONICS RESEARCH
& DEVELOPMENT COMMAND
ATTN TECHNICAL DIRECTOR, DRDEL-CT

HARRY DIAMOND LABORATORIES
ATTN CO/TD/TSO/DIVISION DIRECTORS
ATTN CHIEF, 11000
ATTN CHIEF, 13000
ATTN CHIEF, 15300
ATTN RECORD COPY, 81200
ATTN HDL LIBRARY, (3 COPIES) 81100
ATTN HDL LIBRARY, (WOODBRIDGE) 81100
ATTN TECHNICAL REPORTS BRANCH, 81300
ATTN CHAIRMAN, EDITORIAL COMMITTEE
ATTN FARRAR, R., 13500
ATTN KARAYIANIS, N., 13200
ATTN KULPA, S., 13300
ATTN LEAVITT, R., 13200
ATTN MORRISON, C., 13200
ATTN WORTMAN, D., 13200
ATTN SATTLER, J., 13200
ATTN SIMONIS, G., 13200
ATTN WORCHESKY, T., 13200
ATTN BROWN, E. A., 00210 (25 COPIES)
ATTN CHIEF, 13300
ATTN TOBIN, M., 13200


FILMED
2-8